Journal of Solid State Chemistry 183 (2010) 1640–1644

Contents lists available at ScienceDirect

Journal of Solid State Chemistry

journal homepage: www.elsevier.com/locate/jssc

$\mathrm{KBi}M\mathrm{S}_4$ (M=Si, Ge): Synthesis, structure, and electronic structure

Dajiang Mei [a,b], Zhesuai Lin [a], Lei Bai [a], Jiyong Yao [a,*], Peizhen Fu [a], Yicheng Wu [a]

[a] *Key Laboratory of Functional Crystals and Laser Technology, Technical Institute of Physics and Chemistry, Chinese Academy of Sciences, Beijing 100190, PR China*
[b] *Graduate University of Chinese Academy of Sciences, Beijing 100049, PR China*

ARTICLE INFO

Article history:
Received 27 February 2010
Received in revised form
26 April 2010
Accepted 2 May 2010
Available online 6 May 2010

Keywords:
Bismuth
Sulfide
Synthesis
Crystal structure
Optical
Band structure

ABSTRACT

Two new bismuth sulfides $\mathrm{KBiSiS_4}$ and $\mathrm{KBiGeS_4}$ have been synthesized by means of the reactive flux method. They adopt the $\mathrm{RbBiSiS_4}$ structure type and crystallize in space group $P2_1/c$ of the monoclinic system. The structure consists of $^{\infty}_{2}[\mathrm{Bi}M\mathrm{S}_4^-]$ (M=Si, Ge) layers separated by bicapped trigonal-prismatically coordinated K atoms. The M atom is tetrahedrally coordinated to four S atoms and the Bi atom is coordinated to a distorted monocapped trigonal prism of seven S atoms. The optical band gap of 2.25(2) eV for $\mathrm{KBiSiS_4}$ was deduced from the diffuse reflectance spectrum. From a band structure calculation, the optical absorption for $\mathrm{KBiSiS_4}$ originates from the $^{\infty}_{2}[\mathrm{BiSiS_4^-}]$ layer. The Si 3*p* orbitals, Bi 6*p* orbitals, and S 3*p* orbitals are highly hybridized near the Fermi level. The orbitals of K have no contributions on both the upper of valence band and the bottom of conduction band.

1. Introduction

Bismuth chalcogenides have received considerable attention due to their amazing structural and compositional complexity [1] and their interesting properties [2–8]. The stereochemical activity of the $6s^2$ lone pair of electrons influences the structure type, the electronic structure, and thus the properties of Bi chalcogenides. In the past 20 years, exploratory research has led to the discovery of many new bismuth chalcogenides with intriguing properties including thermoelectric and nonlinear optical properties [6–8]. Many recent reports on bismuth chalcogenides have focused on generating non-centrosymmetric (NCS) structures since $\mathrm{Bi^{3+}}$ is susceptible to the second-order Jahn-Teller effect owing to the $6s^2$ lone pair of electrons [8–13]. The combination of $\mathrm{Bi^{3+}}$ with cations in tetrahedral coordination geometry often results in NCS structures. Examples include the compounds $\mathrm{Cs_5BiP_4Se_{12}}$ [8] $A\mathrm{Bi_2CuS_4}$ (A=K, Cs) [9,10], $\mathrm{KBiP_2S_6}$ [11], $\mathrm{K_9Bi(PS_4)_4}$ [12], and $\mathrm{Cu_2Pb_2Bi_6S_{12}}$ [13]. NCS compounds are of great interest because they may possess technologically important properties, such as the piezoelectric, ferroelectric, and nonlinear optical (NLO) properties [14]. For example, the compound $\mathrm{Cs_5BiP_4Se_{12}}$ exhibits very large second harmonic generation signals [8].

In the $A/M/\mathrm{Bi}/Q$ (A=alkali metal; M=Si, Ge; Q=chalcogen) system, four compounds, namely $\mathrm{RbBiSiS_4}$, $\mathrm{RbBiGeS_4}$, $\mathrm{CsBiSiS_4}$, and $\mathrm{CsBiGeS_4}$ have been reported [15]. Unfortunately, they all adopt centrosymmetric structures although the $\mathrm{Bi^{3+}}$ cations possess a structurally active lone pair of electrons and Si and Ge adopt tetrahedral coordination in the structures. However several reports have shown that the size of the alkali metal has great influence on the crystal symmetry. For example, $\mathrm{LiAsS_2}$ is non-centrosymmetric while $\mathrm{NaAsS_2}$ is centrosymmetric and the non-centrosymmetric structure of $\mathrm{Li_{1-x}Na_xAsS_2}$ holds up to 40% sodium [16]. Another example is the $A_3\mathrm{Ta_2AsS_{11}}$ (A=K, Rb, Cs) series of compounds: the larger $\mathrm{Cs^+}$ favors the centrosymmetric packing of the $^{\infty}_{1}[\mathrm{Ta_2AsS_{11}^{3-}}]$ polymeric anionic chains, while the smaller $\mathrm{Rb^+}$ and $\mathrm{K^+}$ cations favor non-centrosymmetric packing [17]. These results inspire us to reinvestigate the $A/\mathrm{Bi}/M/Q$ (A=alkali metal, M=Si, Ge; Q=chalcogen) with emphasis on smaller alkali metals (i.e. K, Na, Li) in the hope of discovering new NCS structure with interesting properties. Our exploration has led to the discovery of two new K compounds, namely $\mathrm{KBiSiS_4}$ and $\mathrm{KBiGeS_4}$. Here we report the synthesis, structure, optical property, and band structure of these two compounds.

2. Experimental section

2.1. Synthesis

The following reagents were used: K (Sinopharm Chemical Reagent Co., Ltd., 98+%), Si (Sinopharm Chemical Reagent Co., Ltd., 99.5%), Ge (Sinopharm Chemical Reagent Co., Ltd., 99.999%), Bi (Sinopharm Chemical Reagent Co., Ltd., 99.999%), and S (Sinopharm Chemical Reagent Co., Ltd., 99.5%). $\mathrm{K_2S_3}$, the reactive

---

* Corresponding author. Fax: +86 10 82543452.
E-mail address: jyao@mail.ipc.ac.cn (J. Yao).

0022-4596/$ - see front matter © 2010 Elsevier Inc. All rights reserved.
doi:10.1016/j.jssc.2010.05.003

flux [18] employed in the synthesis, was prepared by stoichiometric reaction of the elements in liquid NH_3. Reaction mixtures of 1 mmol of K_2S_3, 1.5 mmol of M (M=Si, Ge), 0.5 mmol of Bi, and 4.8 mmol of S were loaded into fused-silica tubes under an Ar atmosphere in a glovebox. These tubes were sealed under a 10^{-3} Pa atmosphere and then placed in a computer-controlled furnace. The samples were heated to 473 K in 20 h, kept at 473 K for 10 h, then heated to 873 K in 24 h, kept at 873 K for 72 h, slowly cooled at 4 K/h to 373 K, and then cooled to room temperature.

The reaction mixtures were washed free of flux with *N*,*N*-dimethylformamide and then dried with acetone. The products consist of red plates of $KBiSiS_4$ and $KBiGeS_4$ with about 40% yield (based on Bi). Analyses of these compounds with an EDX-equipped Hitachi S-3500 SEM showed the presence of K, M, Bi, and S. The compounds are moderately stable in air. Analysis of the byproducts indicated that they were mainly ternary A/Bi/S compounds.

2.2. Structure determination

Single-crystal X-ray diffraction data were collected with the use of graphite-monochromatized Mo $K\alpha$ radiation (λ=0.71073 Å) at 93 K on a Rigaku AFC10 diffractometer equipped with a Saturn CCD detector. Crystal decay was monitored by re-collecting 50 initial frames at the end of data collection. The collection of the intensity data was carried out with the program Crystalclear [19]. Cell refinement and data reduction were carried out with the use of the program Crystalclear [19], and face-indexed absorption corrections were performed numerically with the use of the program XPREP [20].

The structures were solved with the direct methods program SHELXS and refined with the least-squares program SHELXL of the SHELXTL.PC suite of programs [20]. Each final refinement included anisotropic displacement parameters and a secondary extinction correction. The program STRUCTURE TIDY [21] was then employed to standardize the atomic coordinates. Additional experimental details are given in Table 1 and selected metrical data are given in Tables 2 and 3. Further information may be found in Supplementary material.

2.3. Diffuse reflectance spectroscopy

A Cary 1E UV–visible spectrophotometer with a diffuse reflectance accessory was used to measure the spectrum of $KBiSiS_4$ over the range 350 nm (3.54 eV)–850 nm (1.46 eV).

Table 1
Crystal data and structure refinements for $KBiSiS_4$ and $KBiGeS_4$ [a].

	$KBiSiS_4$	$KBiGeS_4$
fw	404.41	448.91
a (Å)	6.4769(13)	6.5981(13)
b (Å)	6.7371(13)	6.8149(14)
c (Å)	17.168(4)	17.284(4)
β (deg)	108.14(3)	108.46(3)
V (Å^3)	711.9(3)	737.2(3)
ρ_c (g/cm^3)	3.773	4.045
μ (cm^{-1})	265.70	294.95
$R(F)$ [b]	0.0147	0.0296
$R_w(F_o^2)$ [c]	0.0281	0.0571

[a] For both structures Z=4, space group=$P2_1/c$, T=93(2) K, and λ=0.71073.

[b] $R(F)=\sum||F_o|-|F_c||/\sum|F_o|$ for $F_o^2>2\sigma(F_o^2)$.

[c] $R_w\left(F_o{}^2\right)=\{\sum[w(F_o{}^2-F_c{}^2)^2]/\sum wF_o{}^4\}^{1/2}$ for all data. $w^{-1}=\sigma^2\left(F_o{}^2\right)+(zP)^2$, where P=(Max(F_o^2, 0)+2F_c^2)/3; z=0.02 for $KBiSiS_4$ and 0.03 for $KBiGeS_4$.

Table 2
Atomic coordinates and equivalent isotropic displacement parameters (Å^2) for $KBiSiS_4$ and $KBiGeS_4$.

Atom	x	y	z	U_{eq}
K	0.21028(13)	0.74518(12)	0.96350(5)	0.01060(18)
Bi	0.73492(2)	0.18058(2)	0.781160(8)	0.00508(5)
Si	0.29847(16)	0.26957(15)	0.84677(6)	0.0049(2)
S1	0.49453(13)	0.01032(13)	0.86274(5)	0.00631(18)
S2	0.08739(14)	0.24036(14)	0.91834(6)	0.00726(19)
S3	0.51388(14)	0.51006(14)	0.87375(5)	0.00720(19)
S4	0.10759(14)	0.31249(13)	0.72050(5)	0.00605(18)
$KBiGeS_4$				
K	0.2875(3)	0.7414(3)	0.03605(11)	0.0180(4)
Bi	0.23494(5)	0.67750(4)	0.282715(18)	0.00816(11)
Ge	0.20436(13)	0.26785(12)	0.15286(5)	0.00669(19)
S1	0.0147(3)	0.0167(3)	0.37413(12)	0.0116(4)
S2	0.4190(3)	0.2317(3)	0.07928(12)	0.0116(5)
S3	0.0019(3)	0.5047(3)	0.36212(12)	0.0100(4)
S4	0.4024(3)	0.3219(3)	0.28254(12)	0.0096(4)

U_{eq} is defined as one third of the trace of the orthogonalized U_{ij} tensor.

Table 3
Selected bond lengths (Å) for $KBiMS_4$ (M=Si, Ge).

	$KBiSiS_4$	$KBiGeS_4$		$KBiSiS_4$	$KBiGeS_4$
M-S1	2.1264(13)	2.180(2)	Bi-S2	2.7518(14)	2.755(2)
M-S2	2.1127(14)	2.196(2)	Bi-S3	2.8846(13)	2.640(2)
M-S3	2.0937(14)	2.216(2)	Bi-S3	3.305(2)	3.347(2)
M-S4	2.1546(15)	2.239(2)	Bi-S4	2.6850(10)	2.664(2)
Bi-S1	2.6570(10)	2.904(2)	Bi-S4	3.0439(11)	3.110(2)
Bi-S1	3.311(2)	3.377(2)			

2.4. Theoretical calculation

The electronic property calculations were performed using the first principles plane-wave pseudopotential method [22] implemented in the CASTEP package [23]. Normal-conserving pseudopotentials [24,25] are adopted with the 1*s*, 2*s*, and 2*p* electrons for potassium, silicon and oxygen treated as core electrons. For bismuth, 5*d*, 6*s*, and 6*p* electrons are chosen as the valence electrons. A kinetic energy cutoff of 700 eV is employed, and the local-density approximation is chosen. Monkhorst–Pack [26] *k* point meshes with a density of (4 × 4 × 2) points in the Brillouin zone of the unit cell are used.

3. Results and discussion

3.1. Synthesis

The synthetic conditions of the title compounds differed from those used in the syntheses of the previously reported $RbBiSiS_4$, $RbBiGeS_4$, $CsBiSiS_4$, and $CsBiGeS_4$ compounds [15]. The S/A_2S_3 (A=K, Rb, Cs) ratio was larger; this less basic reaction condition is important for the crystallization of the two K compounds. The yield was about 40% in the synthesis, which was not improved much after several different trials. The other 60% were black noncrystalline melt consisting of ternary A/Bi/S compounds, based on EDX. No powder diffraction data were measured on the black melt since they would not provide much information. Efforts to synthesize the Na and Li analogues were unsuccessful, presumably because the Na^+ and Li^+ cations are too small to sustain the anionic framework in the structure.

3.2. Structure

KBiMS$_4$ (M=Si, Ge) crystallizes in RbBiSiS$_4$ structure type [15]. There are no S–S bonds or any detectable disorder among M, Bi, or K atoms in the structure; thus, the oxidation states of 1+, 4+, 3+, and 2− can be assigned to K, M, Bi, and S, respectively.

The structure of KBiMS$_4$ (M=Si, Ge) is illustrated in Fig. 1. It consists of ${}^{\infty}_{2}[\mathrm{Bi}MS_4^-]$ (M=Si, Ge) layers separated by K atoms. Each K atom is coordinated to a bicapped trigonal prism of eight S atoms. The K–S bond lengths range from 3.2058(14) to 3.5239(14) Å in KBiSiS$_4$ and from 3.194(3) to 3.601(3) Å in KBiGeS$_4$. Each M atom is coordinated to a slightly distorted tetrahedron of four S atoms. The M–S bond lengths range from 2.0937(14) to 2.1546(15) Å in KBiSiS$_4$ and from 2.180(2) to 2.239(2) Å in KBiGeS$_4$ (Table 3). Each Bi atom is coordinated by seven S atoms. The coordination geometry may be described as a distorted monocapped trigonal prism comprising five close S atoms at the corners of a square pyramid with Bi near the center of the basal plane and the sixth and seventh S atoms further away (Fig. 2). The S atom at the apex of the square pyramid is the cap of the prism. The largest differences in Bi–S bond lengths within these BiS$_7$ polyhedra are 0.654(1) Å in KBiSiS$_4$ and 0.737(2) Å in KBiGeS$_4$. Earlier calculation has shown that the two longest Bi–S bonds are mainly ionic in character [15]. This kind of coordination geometry is common for Bi atom, for example in CsBi$_3$S$_5$ [27], where the Bi–S bond lengths range from 2.598(3) to 3.178(4) Å for Bi1 and from 2.640(3) to 3.211(4) Å for Bi2. Although the Bi^{3+} cation contains a stereoactive lone pair of electrons, the position of this lone pair is not apparent, either from the distortion of the Bi coordination sphere or from the X-ray diffraction data.

The structure of the ${}^{\infty}_{2}[\mathrm{BiSiS}_4^-]$ layer in KBiSiS$_4$ is shown in Fig. 3. The neighboring BiS$_7$ polyhedra share opposite edges of the rectangular planes of the prisms to form zigzag chains along the b direction (purple lines). Two parallel polyhedral chains are connected by the sharing of opposite edges of the SiS$_4$ tetrahedra. Each SiS$_4$ tetrahedron is arranged in such a way that one of the S atoms becomes the cap of an adjacent BiS$_7$ polyhedron (blue lines). Although the caps in a single layer point in the same direction along the b axis, the caps of neighboring layers point in alternating directions. The structure of the ${}^{\infty}_{2}[\mathrm{BiSiS}_4^-]$ layer in the KBiSiS$_4$ is similar to that of ${}^{\infty}_{2}[\mathrm{BiSiS}_4^-]$ layer in CsBiSiS$_4$ shown in Fig. 4 and the structure of the ${}^{\infty}_{2}[LnMS_4^-]$ layer in the $ALnM$S$_4$ (A=alkali metal, Ln=rare earth; M=Si, Ge) series of compounds [28–39]. The differences between the structures of KBiSiS$_4$ and CsBiSiS$_4$ (Fig. 3 vs. Fig. 4) include the disposition of the capping S atoms (blue lines) and the connectivity between BiS$_7$ polyhedra. In the CsBiSiS$_4$ structure the caps on two sides of a chain point in the same direction along b axis but the caps on neighboring chains in the same layer point in alternating directions and each BiS$_7$ polyhedron in one chain is connected to another BiS$_7$ polyhedron

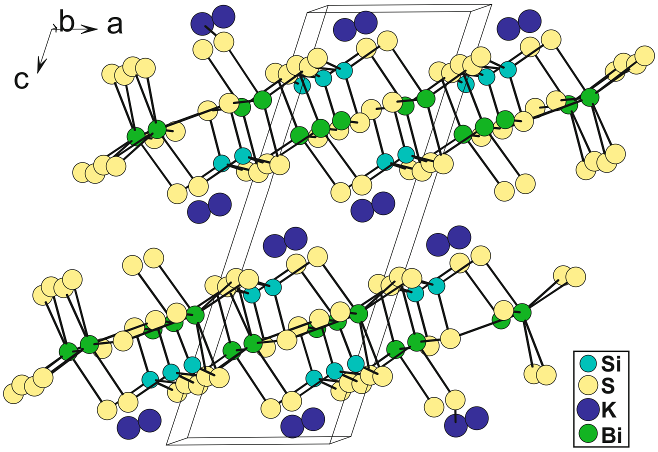

Fig. 1. Unit cell of the KBiSiS$_4$ structure type viewed along [010].

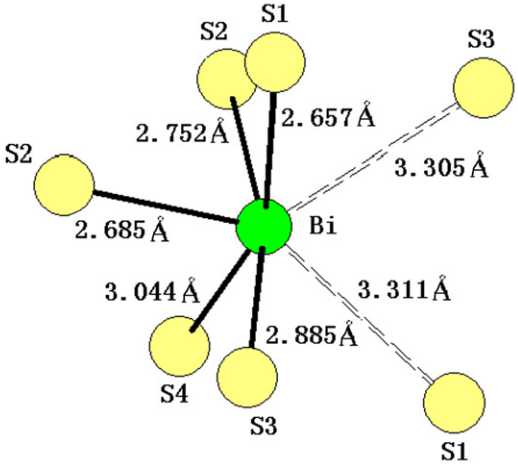

Fig. 2. Coordination geometry of Bi in KBiSiS$_4$ (the dashed hollow lines represent the two longest Bi–S bonds, which are more ionic in character).

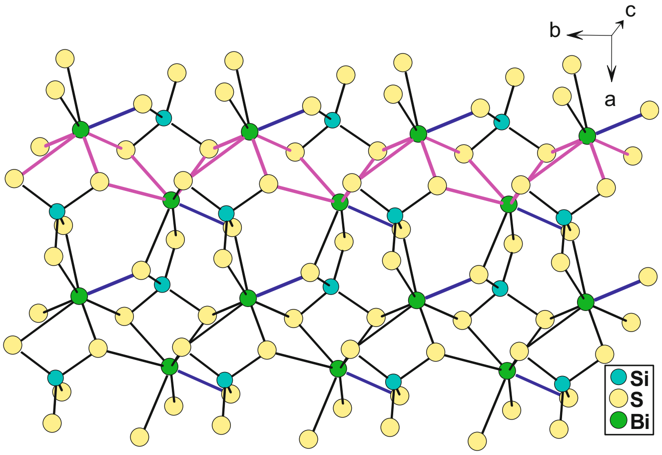

Fig. 3. Structure of the ${}^{\infty}_{2}[\mathrm{BiSiS}_4^-]$ layer in KBiSiS$_4$. Here and in Fig. 4 the blue lines show the capping S atoms and the purple lines display the connectivity between BiS$_7$ polyhedra within a chain. (For interpretation of the references to colour in this figure legend, the reader is referred to the web version of this article.)

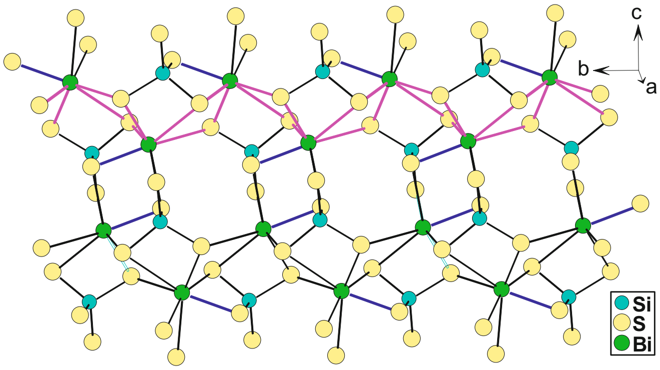

Fig. 4. Structure of the ${}^{\infty}_{2}[\mathrm{BiSiS}_4^-]$ ADVANCE \l 4 layer in CsBiSiS$_4$. (For interpretation of the references to colour in this figure legend, the reader is referred to the web version of this article.)

in a neighboring chain by edging sharing, while in the $KBiSiS_4$ structure all the caps within the layer point in the same direction and the connection between BiS_7 polyhedra is by corner sharing.

In the $ALnMS_4$ (A=alkali metal, Ln=rare earth; M=Si, Ge) series of compounds, the two common structure types are represented by $KLaGeS_4$ (space group $P2_1$) [33] and $CsSmGeS_4$ (space group $P2_12_12_1$),[34] while β-$KCeSiS_4$ (space group $P2_1/m$) [36] and $CsCeSiS_4$ (space group $Pnma$) [39] adopt the other two less common structure types. In contrast to $KBiSiS_4$, the $ALnMS_4$ compound exhibit much smaller differences in the Ln–S bond lengths within the LnS_n (n=7, 8) polyhedra. For example, the largest difference is 0.225(1) Å in $KLaGeS_4$ and 0.185(1) Å in $CsSmGeS_4$. Furthermore, in $KLaGeS_4$ the caps of neighboring layers point in the same direction along the polar b axis, whereas in $CsSmGeS_4$ the two $[SmGeS_4^-]$ slabs in the unit cell are related by a 2_1 screw axis along c rather than a center of inversion. For the two centrosymmetric β-$KCeSiS_4$ and $CsCeSiS_4$ structures, all cations are in positions of m symmetry and the rare-earth cations are in an environment of bicapped trigonal prism. The obvious difference between these two structures and the $KBiSiS_4$ structure lies in the coordination of the capping S atom. In both β-$KCeSiS_4$ and $CsCeSiS_4$, the capping S atoms are in an environment of m symmetry and shared by two Ln atoms, while in $KBiSiS_4$, the capping S is in a general position and is only connected to one Bi atom.

So far, six members of the $ABiMS_4$ family (A=alkali metal, M=Si, Ge) have been found. For the five isostructural compounds, namely $KBiSiS_4$, $RbBiSiS_4$, $KBiGeS_4$, $RbBiGeS_4$, and $CsBiGeS_4$, the $^{\infty}_{2}[BiMS_4^-]$ layers lie within the ab plane and are separated by the A cations along c direction; thus, the a and b dimensions of the unit cell are mainly determined by the M, Bi and S atom while the alkali metal A mainly influence the cell dimension along c direction. In these five members, the a and b axes of compounds containing the same M are quite similar, so do the c axes of compounds containing the same A. On the other hand, the combination of the largest A(Cs) with the smallest M(Si) leads to the formation of a different structure: $CsBiSiS_4$. Clearly, the relative sizes of cations have significant influence on the packing of atoms.

3.3. Experimental band gap

The diffuse reflectance spectrum of $KBiSiS_4$ is shown in Fig. 5. A band gaps of 2.25(2) eV was deduced by the straightforward extrapolation method [40].

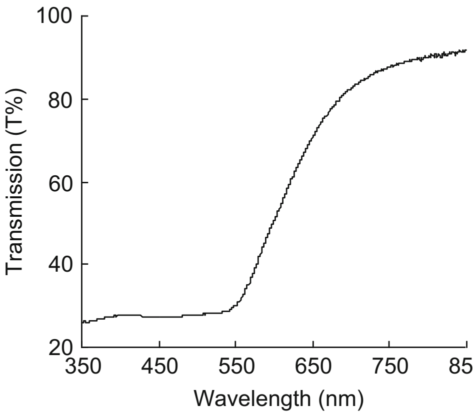

Fig. 5. Diffuse reflectance spectrum of $KBiSiS_4$.

3.4. Band structure calculation

The calculated band structures of the $KBiSiS_4$ crystal in the unit cell are plotted along the symmetry lines in Fig. 6. Obviously, the energy band can be divided into three regions; the lower region is located below −5 eV, the middle region is the valence band (VB) from about −5 to 0 eV, and the upper one is the conduction band (CB) in which a band of a dispersion spanning about 0.6 eV appears at the bottom of its conduction bands on the B point. The calculated indirect band gap is 2.022 eV. This value is a bit smaller than the experimental optical band gap, which is usual for indirect semiconductors. The further calculations with other kinds of pseudopotentials show that the change of the results is not apparent.

Fig. 7 gives the partial DOS (PDOS) projected on the constitutional atoms of the $KBiSiS_4$ crystal, in which several electronic characteristics can be seen: (i) The K 3s orbitals and the Bi 5d orbitals are localized at −28 and −22 eV (not shown), respectively, in the very deep region of the VB; they are not included in the atomic bonds. (ii) The VB from −15 to −5 eV mainly consist of the K 4p, Bi 6s, Si 3s and S 3s orbitals. At the very top of the VB (from 0 to −5 eV), there is quite strong hybridization among the p orbitals of Bi, Si, and S atoms, but the S 3p orbitals occupy the VB maximum. The orbitals of potassium have no contributions on

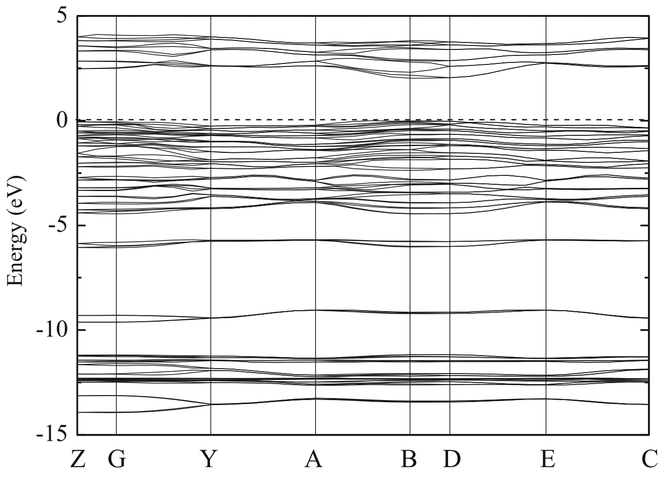

Fig. 6. Band structure of $KBiSiS_4$.

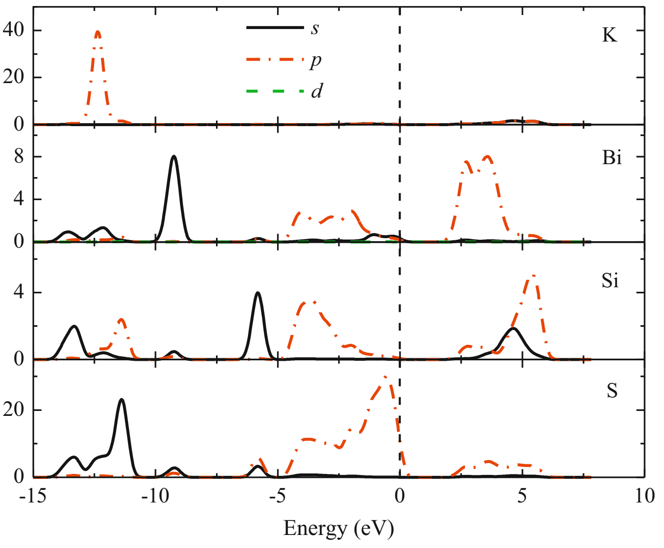

Fig. 7. Partial density of states of $KBiSiS_4$.

both the upper of VB and the bottom of CB. (iii) The CB are mainly composed of the orbitals of Bi, Si and S atoms, but the bottom of CB is determined by the Bi 6*p* orbitals. Moreover, it is found that some Si 3*s* orbitals are unoccupied and located at about 4.3 eV due to the sp^3 hybridization in the $(SiS_4)^{4-}$ group.

Acknowledgment

This research was supported by the National Basic Research Project of China (No. 2010CB630701). ZSL acknowledges the Special Foundation of President of Chinese Academy of Sciences.

Appendix A. Supporting information

Supplementary data associated with this article can be found in the online version at doi:10.1016/j.jssc.2010.05.003.

References

[1] E. Makovicky, Neues Jahrb. Mineral. Abh. 160 (1989) 269.
[2] L.R. Testardi Jr., J.N. Bierly, F.J. Donahoe, J. Phys. Chem. Solids 23 (1962) 1209.
[3] J.D. Feichtner, G.W. Roland, Appl. Opt. 11 (1972) 993.
[4] S. Ibuki, S. Yoschimatsu, J. Phys. Soc. Jpn. 10 (1955) 549.
[5] H. Kaibe, Y. Tanaka, M. Sakata, I. Nishida, J. Phys. Chem. Solids 50 (1989) 945.
[6] D.-Y. Chung, T. Hogan, P. Brazis, M. Rocci-Lane, C. Kannewurf, M. Bastea, C. Uher, M.G. Kanatzidis, Science 287 (2000) 1024.
[7] M.G. Kanatzidis, T.J. McCarthy, T.A. Tanzer, L.-H. Chen, L. Iordanidis, T. Hogan, C.R. Kannewurf, C. Uher, B. Chen, Chem. Mater. 8 (1996) 1465.
[8] I. Chung, J.-H. Song, J.I. Jang, A.J. Freeman, J.B. Ketterson, M.G. Kanatzidis, J. Am. Chem. Soc. 131 (2009) 2647.
[9] Y.-T. Yang, P. Brazis, C.R. Kannewurf, J.A. Ibers, J. Solid State Chem. 155 (2000) 243.
[10] F.Q. Huang, K. Mitchell, J.A. Ibers, J. Alloys Compd. 325 (2001) 84.
[11] V. Manriquez, A. Galdamez, D. Ruiz Leon, M.T. Garland, M. Jimenez, Z. Kristallogr., NCS 218 (2003) 151.
[12] M.A. Gave, D.P. Weliky, M.G. Kanatzidis, Inorg. Chem. 46 (2007) 11063.
[13] D. Topa, V. Petricek, M. Dusek, E. Makovicky, T. Balic-Zunic, Can. Mineral. 46 (2008) 525.
[14] J.F. Nye, in: Physical Properties of Crystals, Oxford University Press, Oxford, 1957.
[15] J. Yao, B. Deng, D.E. Ellis, J.A. Ibers, Inorg. Chem. 41 (2002) 7094.
[16] T.K. Bera, J.-H. Song, A.J. Freeman, J.I. Jang, J.B. Ketterson, M.G. Kanatzidis, Angew. Chem. Int. Ed. 47 (2008) 7828.
[17] T.K. Bera, J.I. Jang, J.B. Ketterson, M.G. Kanatzidis, J. Am. Chem. Soc. 131 (2009) 75.
[18] S.A. Sunshine, D. Kang, J.A. Ibers, J. Am. Chem. Soc. 109 (1987) 6202.
[19] CrystalClear, Rigaku Corporation, Tokyo, Japan, 2008.
[20] G.M. Sheldrick, Acta Crystallogr. Sect. A: Found. Crystallogr. 64 (2008) 112.
[21] L.M. Gelato, E. Parthé, J. Appl. Crystallogr. 20 (1987) 139.
[22] M.C. Payne, M.P. Teter, D.C. Allan, T.A. Arias, J.D. Joannopoulos, Rev. Mod. Phys. 64 (1992) 1045.
[23] S.J. Clark, M.D. Segall, C.J. Pickard, P.J. Hasnip, M.J. Probert, K. Refson, M.C. Payne, Z. Kristallogr. 220 (2005) 567.
[24] A.M. Rappe, K.M. Rabe, E. Kaxiras, J.D. Joannopoulos, Phys. Rev. B 41 (1990) 1227.
[25] J.S. Lin, A. Qtseish, M.C. Payne, V. Heine, Phys. Rev. B 47 (1993) 4174.
[26] J.P. Perdew, K. Burke, M. Ernzerhof, Phys. Rev. Lett. 77 (1996) 3865.
[27] A.S. Kanisheva, Y.N. Mikhailov, B.V. Lazarev, A.F. Trippel, Dok. Akad. Nauk SSSR 252 (1980) 96.
[28] G. Gauthier, F. Guillen, S. Jobic, P. Deniard, P. Macaudiere, C. Fouassier, R. Brec, C.R. Acad. Sci. Paris, T. 1, Ser. II 2 (1999) 611.
[29] I. Hartenbach, T. Schleid, Z. Anorg. Allg. Chem. 631 (2005) 1365.
[30] A. Choudhury, L.A. Polyakova, I. Hartenbach, T. Schleid, P.K. Dorhout, Z. Anorg. Allg. Chem. 632 (2006) 2395.
[31] S.P. Guo, H.Y. Zeng, G.C. Guo, J.P. Zou, G. Xu, J.S. Huang, Chin. J. Struct. Chem. 27 (2008) 1543.
[32] C.R.I.V. Evenson, P.K. Dorhout, Inorg. Chem. 40 (2001) 2409.
[33] P. Wu, J.A. Ibers, J. Solid State Chem. 107 (1993) 347.
[34] C.K. Bucher, S.-J. Hwu, Inorg. Chem. 33 (1994) 5831.
[35] I. Hartenbach, T. Schleid, Z. Anorg. Allg. Chem. 629 (2003) 394.
[36] I. Hartenbach, T. Schleid, Z. Anorg. Allg. Chem. 628 (2002) 1327.
[37] B.C. Chan, P.K. Dorhout, Z. Kristallogr. NCS 220 (2005) 7.
[38] A.K. Gray, J.M. Knaust, B.C. Chan, L.A. Polyakova, P.K. Dorhout, Z. Kristallogr. NCS 220 (2005) 293.
[39] I. Hartenbach, T. Schleid, Z. J. Alloys Compd. 418 (2006) 95.
[40] O. Schevciw, W.B. White, Mater. Res. Bull. 18 (1983) 1059.